STRUCTURAL EVOLUTION OF THE NORTHERN SUB-ANDES OF ECUADOR: THE NAPO UPLIFT

Wilfrido. BALSECA(1), Luca FERRARI(2), Giorgio PASQUARE'(2) and Alessandro TIBALDI(2)

(1)Instituto Ecuatoriano de Electrificacion (INECEL), Division Ingenieria y Geotecnica, Av. 6 de Diciembre 2275 y Av. Orellana, Casilla 585 - A, Quito, Ecuador
(2)Dipartimento Scienze della Terra, Università di Milano, Via Mangiagalli 34, 20133 Milan, Italy

Resumen

La Zona Subandina ecuatoriana està formada por los dos levantamientos estructurales regionales del Cutucù al Sur y del Napo al Norte, separados entre sì por la depresiòn del Pastaza. La evoluciòn tectonica del Levantamiento del Napo ha sido estudiada por medio de un levantamento geologico regional y estructural a la escala 1: 50.000 integrado por datos de subsuelo proporcionados por Petroecuador e INECEL. El Levantamiento Napo resulta ser formado por una faja de escamas semimetamorficas y cabalgamientos, un combamiento regional afectados por fallas trascurrentes y una flexura. Estas estructuras se han formado en tres etapas pricipales de deformaciòn desde el Cretacico superiòr hasta el presente.

Key Words: Ecuador, sub-Andes, Napo uplift, tectonics, structural evolution

Introduction

The sub-andean zone of Ecuador is a NNE trending deformed belt which connect the higher "Sierra" region to the west with the lowlands of the Amazonian foreland to the east. The sub-andes are formed by two structural highs, known as Cutucù and Napo uplifts, which are separated by the Pastaza depression. The "Sierra" is formed by the parallel ranges of Cordillera Real (CR) and Cordillera Occidental (CO), which are considered allochtonous terranes accreted onto the South American margin during two major tectonic phase in early Createaceous and early Tertiary times respectively (Wallrabe-Adams, 1990). The CR is made of cristalline rocks dating back to Paleozoic and early Mesozoic which undergone several orogenic phases since early Triassic (Baldock, 1982). In early Cretaceous this terrane has been metamorphosed, often dynamically, (Litherland and Aspden, 1992) while during Tertiary has been thrusted onto the Sub-Andean zone with a ESE vergence. (Pasquarè et al., 1990).

In this work we present a new synthesis on the tectonic evolution of the Napo uplift which is the result of six years of stratigraphic and structural studies in the northern sub-Andes of Ecuador. This work is based on an extensive geologic mapping of the whole Napo uplift and parts of the adjoining areas (Balseca and Pasquarè, in press) integrated with subsurface geologic data kindly made available by Petroecuador and INECEL. The new data depict a tectonic evolution characterized by rapid changes in the deformation styles and a strong rigidity of the whole rock masses. The structure of the Napo uplift is more complex than previously reported, being formed by the justapoxition of embricated thrust slices, strike-slip faults and flexures.

Structural setting

The Napo uplift is a 70km-wide, 150km-long positive structure which has a structural relief of about 1.6 km with respect to the Amazonian foreland. The core of the Napo uplift is made of Jurassic to Cretaceous sedimentary and volcanic rocks (Misahualli, Hollin, Napo and Tena Formations), with a general sub-horizontal attitude and, to the west, by various granitoids of Jurassic age (Abitagua, Cuchilla), emplaced with a NNE trending alignment. All these rocks are cut mainly by NNE to NE trending right-lateral strike-slip faults and, to a lower extent, by NNW-SSE left-lateral faults. The NNE and NE faults show sometimes a vertical component of motion particularly where the two set of faults converge to give rise to restraining bands which contribute to produce the central culmination of the Napo uplift. At a regional scale the maximum elevation of the Napo uplift is located along a NNW-SSE trending axis passing through the Sumaco volcano. The southern sector is characterized by some kilometric folds trending from N-S to NNE.

Toward the west, approaching the CR, the sub-horizontal attitude of the core strata turns to a more complicated arrangement. Jurassic-Cretaceous formations are involved in WNW dipping thrust slices which display a dynamic metamorphism and both ductile and brittle deformations. These rocks are exposed in a NNE trending belt which is cut by NE trending right-lateral strike-slip faults. Blocks of the CR are thrusted along W and WNW dipping reverse and right-lateral reverse faults over the dinamometamorphosed belt producing a relatively lowering of this zone with respect to the CR and the central Napo core. Such a topographic situation has previously suggested the existence of a western flank of a large Napo anticline.

In the northern sector, the limit with the Amazonian foreland is a wide flexure where Cretaceous to Miocene strata dip 50° up to 70° eastwards. This structure is interpreted as the surface manifestation of a blind thrust, which has been encountered at least in one site by an oil well (Rivadeneria and Ramirez, 1985). The flexure is furtherly complicated by several NE trending right-lateral strike-slip faults which coincide with large deformations of its geometry. Southwards, the flexure disappears and the Napo uplift is truncated by a system of NE striking right-lateral strike-slip faults.

Further to the south the Pastaza depression is characterized by N-S trending reverse faults and folds while its limit with the Amazonian plain is an arcuate thrust buried underneath the Plio-Quaternary alluvium.

Age of faulting

Although many tectonic phases can be recognized in the study area, we focussed on the late Cretaceous to Quaternary tectonic history which is responsible for the formation of the Napo uplift. The first pulse in this tectonic cycle evidenced by the erosion of the upper part of the Napo Formation during the Campanian. Among the main structures of the Napo uplift the N-S to NNE-SSW trending reverse faults resulted to be the oldest structures, in agreement with previous works in the CR (Pasquarè et al., 1990). These faults absorbed most of the shortening which accompanied the formation of the dynamometamorphic slice belt. The age of the rocks involved in this belt constrained to the Paleogene the developing of this structure. Later, the N-S to NNE-SSW fault planes were partially rejuvenated with right-lateral reverse motions. The NNW trending left-lateral strike-slip faults are older than the NNE to NE trending right-lateral strike-slip faults because are systematically displaced by the latter but no absolute age is available for the formation of the former. Quaternary alluvial deposits of the Amazonian plain onlap the flexure and are generally undeformed. Nevertheless, they locally show remote-sensed lineaments which may suggest an extension of the transcurrent faulting towards the east. Finally, motions along the NE to NNE trending right-lateral strike-slip faults occurred during the Quaternary as witnessed by morphological neotectonic indicators and seismicity analyses (Tibaldi and Ferrari, 1992).

Tectonic evolution

Field data suggest that the Napo uplift developed during three main stages of deformation since Paleogene times, although the first upraise of the region begun in late Cretaceous. In a first stage, occurred between Paleogene and Miocene, the CR was thrusted toward the ESE onto the western side of the Napo area producing the dynamometamorphic slice belt. In a second stage, the eastward propagation of deformation produced the regional arching and the flexure which limits the eastern flank of the Napo uplift. During this second stage, N-S to NNE right-lateral reverse faults developed within the dynamometamorphic slice belt, while NNW left-lateral and NE right-lateral faults developed eastwards. We think that this stage could correspond to the Neogene time. During the third stage, in the Quaternary, right-lateral transcurrent motions along NE to NNE trending faults cut the Napo uplift into four main blocks. These blocks were differentially thrusted toward the NE creating in the distortion and the truncation of the flexure.

ACKNOWLEDGMENTS

We thanks Instituto Ecuatoriano de Electrificacion (INECEL) Quito, for the logistical support in the field works and for the continuous sustaining of W.B. throughout the study. We also acknowledge Petroecuador for the kind permission of studying subsurface data.

W.B. and L.F. benefited of a grants of Consorzio Milano Ricerche. A.T. was partially supported by a Ph.D. grant from Ministero Italiano della Pubblica Istruzione.

REFERENCES

Aspden J.A. and Litherland M., 1992. The geology and Mesozoic collisional history of the Cordillera Real, Ecuador. Tectonophysics, 205, 187-204.

Baldock J. W., 1982. Geologia del Ecuador (Boletin de la explicaciòn y mapa geologico de la Republica del Ecuador, escala 1 : 1,000,000). Direcciòn General de Geologia y Minas, Quito, 71 pp.

Balseca W. and Pasquarè G. Regional geologic map of the Napo uplift, northeastern Ecuador. Acta Vulcanologica, in press.

Pasquarè G., Tibaldi A. and Ferrari L., 1990. Relationships between plate convergence and tectonic evolution of the Ecuadorian active Thrust Belt. In: Agusthithis S.S. (Ed.), Critical Aspects of Plate Tectonic Theory, Theophrastus Publications, 365-387.

Rivadeneria M.V. and Ramirez F.H., 1985. La zona subandina amazonica ecuatoriana y sus prospectos hidrocarburiferos. VI° Latinamerican geological congress, Bogotà, Colombia.

Tibaldi A. and Ferrari L., 1992. Latest Pleistocene-Holocene tectonics of the Ecuadorian Andes. Tectonophysics, 205, 109-125.

Wallrabe-Adams H., 1990. Petrology and geotectonic development of the Western Ecuadorian Andes: the Basic Igneous Complex. Tectonophysics, 185, 163-182.

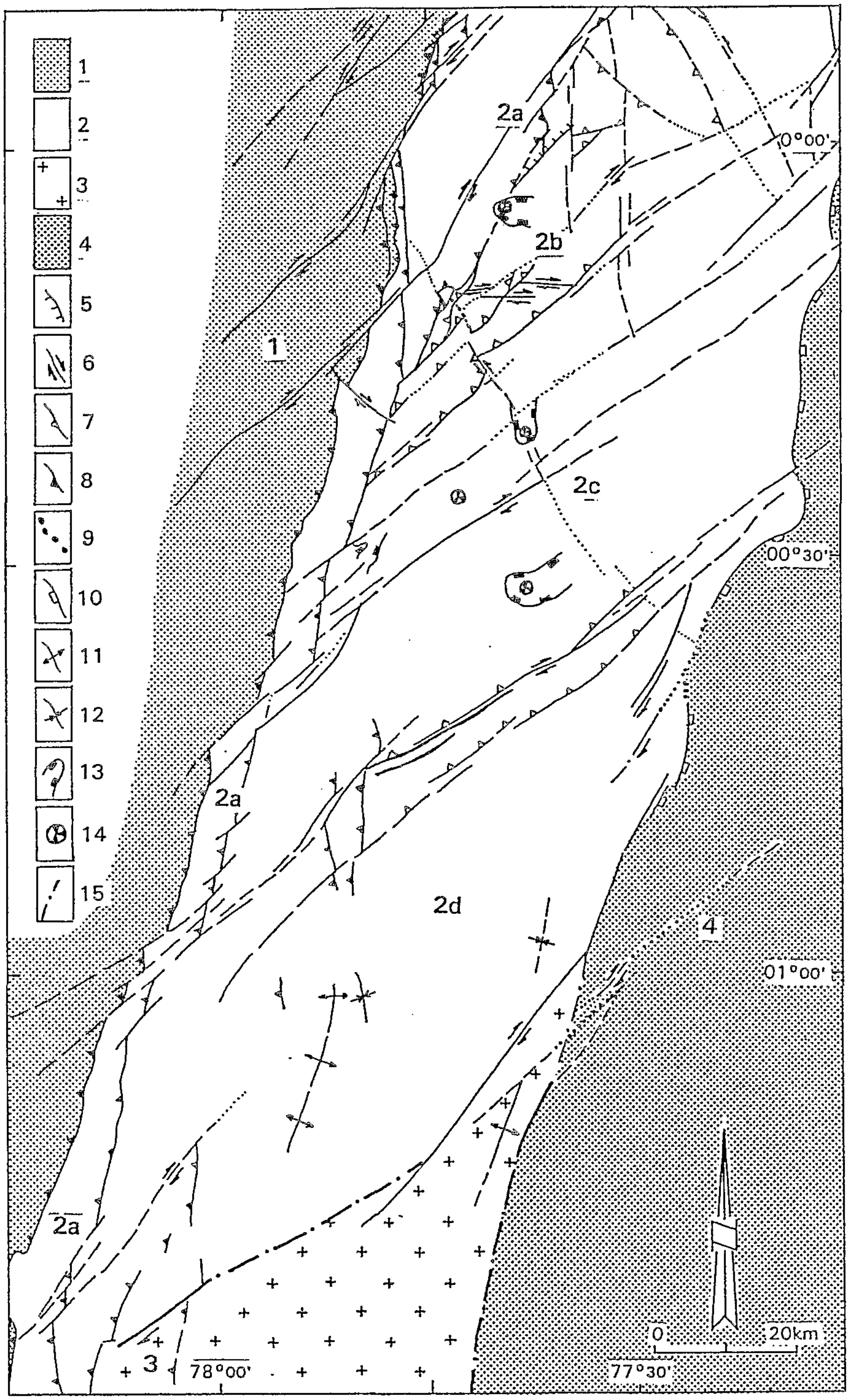

Figure 1. Structural sketch-map of the Napo uplift.
1 = Polimetamorphic rocks of the Cordillera Real. 2 = Napo uplift: a) thrust slice zone; b) zone with strike-slip and reverse faults; c) zone with strike-slip faults; d) zone with strike-slip and folds. 3 = Pastaza depression. 4 = Amazonian foreland. 5 = normal faults. 6 = Strike-slip faults. 7 = reverse faults. 8 = Thrusts. 9 = buried faults. 10 = flexure. 11= anticline fold axis. 12 = sycline fold axis. 13 = volcanic collapse. 14 = volcanic vent. 15 = inferred faults.